Science Press

Trans. Nonferrous Met. Soc. China 17(2007) s198−s203

Transactions of Nonferrous Metals Society of China

www.csu.edu.cn/ysxb/

Morphology and corrosion resistance of composite coatings obtained by phosphating and molybdate post-sealing on galvanized steel

XU Yu-ye(徐玉野)[1], LIN Bi-lan(林碧兰)[2], LU Jin-tang(卢锦堂)[2]

1. College of Civil Engineering, Huaqiao University, Quanzhou 362021, China;
2. College of Materials Science and Engineering, South China University of Technology, Guangzhou 510640, China

Received 15 July 2007; accepted 10 September 2007

Abstract: The phosphated hot-dip galvanized (HDG) sheets were post-sealed with sodium molybdate solution to improve the corrosion resistance of phosphate coatings. The morphology, chemical composition and corrosion resistance of the coatings were investigated using scanning electron microscopy (SEM), energy dispersive spectroscopy (EDS), Tafel polarization measurements and neutral salt spray (NSS) tests, and were compared with those of the single coatings. The results show that post-sealing the phosphated HDG steel with molybdate solution, the pores among the zinc phosphate crystals are sealed with molybdate films containing Zn, P, O and Mo, and the continuous composite coatings are formed. The suppression of both the anodic and the cathodic processes of zinc corrosion on the samples are enhanced significantly. The synergistic corrosion protection effect of the single phosphate coatings and molybdate films for zinc is evident. The corrosion resistance of the composite coatings increases with phosphating time up to 300 s.

Key words: galvanized steel; phosphate coatings; molybdate; corrosion resistance; polarization curve

1 Introduction

Hot dip galvanizing is an effective protection measure for steel against atmospheric corrosion. And phosphating is one of the most important chemical conversion processes for corrosion protection or painting primer for the galvanized layers. However, phosphate coatings are crystalline and porous, which requires a post-treatment after phosphating[1−3].

A mixture of hexavalent and trivalent chromate, or dilute chromic acid solutions have been used traditionally for the post-sealing treatment[1−4]. The serious environmental difficulties connected with chromate promote the development of chrome-free alternatives[4−5], but few chrome-free approaches provide the same corrosion resistance as that of chromate. Nevertheless, some new post-sealing methods that can achieve comparable corrosion protection to that provided by chromate have also been reported [4, 6]. NIE et al[6] have reported that the corrosion resistance offered by the methyltrimethoxy silane (MS)/Zr post-sealing is better than that provided by the chromate on the zinc-phosphated hot-dip galvanized(HDG) steel using EIS measurements.

Molybdate is an environmentally acceptable and effective corrosion inhibitor for zinc, galvanized steel and other metals[7−8]. Molybdate conversion films for different substrates have been documented[9−10]. Molybdate films are amorphous, but they have cracks during a longer immersion[9]. Molybdate additives to a phosphate solution to accelerate the phosphating processes or to improve the corrosion resistance of phosphate coatings have also been reported[11−14]. Nevertheless, molybdate additives could not make the pores on phosphate coatings to be eliminated thoroughly. In this study, the phosphated HDG samples were post-sealed with molybdate solution. The effect of molybdate post-sealing on the morphology and corrosion resistance of phosphate coatings was investigated.

2 Experimental

Q235 cold-rolled sheets (50 mm×40 mm×2 mm) were degreased, pickled, fluxed, dried and dipped in a zinc bath at 450 ℃ for 1 min, then withdrawn slowly and quenched in water immediately. The thickness of the

Foundation item: Project(07BS405) supported by the Excellent Talents Foundation of Huaqiao Univeristy, China
Corresponding author: XU Yu-ye; Tel: +86-13665961191; E-mail: yuyexu@hqu.edu.cn

galvanized layer was about 50 μm.

In the previous study[9, 15], the respective process technologies for phosphating and molybdate treatment applied to HDG steel are shown in Table 1. The optimal immersion time for molybdate conversion films was 50 s[9]. In this study, the process technologies for phosphating and molybdate post-sealing treatment were also chosen in Table 1. The solutions were prepared from reagent grade chemicals and de-ionized water.

Table 1 Process technologies for phosphating and molybdate treatment

Phosphating	Molybdate treatment
ZnO: 1.2 g/L	$Na_2MoO_4·2H_2O$: 10 g/L
$NaNO_3$: 15 g/L	$Na_3PO_4·12H_2O$: 10 g/L
85% H_3PO_4: 11 mL/L	H_3PO_4: proper
Temperature: 45 ℃	Temperature: 60 ℃
pH: 3.0	pH: 4.6
Time: 2−600 s	Time: 10−180 s

Tafel polarization measurements were carried out under CHI604B electrochemical workstation with a conventional three-electrode cell system in 5% NaCl solution at room temperature. A saturated calomel electrode (SCE) was used as a reference electrode. A platinum electrode of 10 cm^2 served as an auxiliary electrode. The exposed area of the working electrode was 1 cm^2. The scan rate for polarization was 1 mV/s.

Neutral salt spray(NSS) tests were conducted using 5% NaCl solution with pH value of 6.5−7.0 at(35±2)℃. The samples were placed perpendicularly with an angle of 30°. In a spray cycle, the samples were continuously sprayed for 8 h and then kept in NSS chamber for 16 h. The corroded area of zinc was recorded after each spray cycle.

The surface morphology of the coated samples was observed by SEM (PHILIPS; Model: XL-30-FEG). The chemical composition of the coatings was analyzed by EDS (EDAX; Model: DX-4).

3 Results and discussion

3.1 Morphology and composition of coatings

SEM results show that the zinc phosphate crystals are already observed on the zinc layer after immersing HDG steel in phosphating solution for 2 s. With the increase in phosphating time, the initial zinc phosphate crystals grow up, the new crystal nuclei deposit and the growth stops until the crystals melt together[15]. The microstructure of the zinc phosphate crystals is needle-like, resulting in the residual pores among the zinc phosphate crystals[15]. The porosity of zinc phosphate coatings on HDG steel measured by linear polarization method decreases with the increase in time at the initial stage of phosphating and followed by stabilizing for phosphating time longer than 300 s[15−16].

Fig.1 shows the SEM micrograph of the 5 s phosphated HDG sample post-sealed with molybdate solution for 10 s and finally without rinse. Two types of the films seem to be formed on the surface of the zinc layer. One type may be the phosphate coatings on which have the needle-like zinc phosphate crystals, and the other type may be the molybdate films which apparently cover the grain boundaries of zinc.

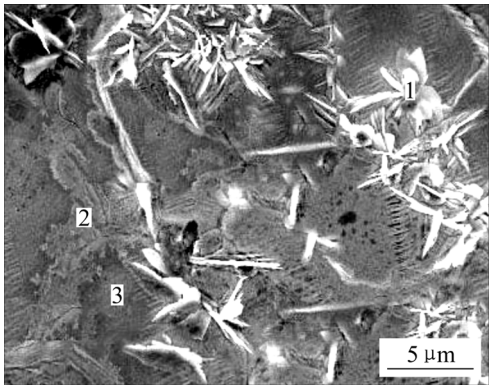

Fig.1 SEM micrograph of 5 s phosphated HDG sample post-sealed with molybdate solution for 10 s

The chemical composition of different micro-sites corresponding to Fig.1 is listed in Table 2. Besides the grain boundaries of zinc, the elements of Zn, P, O and Mo are detected on the surfaces of both the needle-like zinc phosphate crystals and the intra-crystallines of zinc. It is suggested that some molybdate compounds cover the needle-like zinc phosphate crystals and molybdate films are also formed at the grain boundaries and intra-crystallines of zinc. The content of Mo at the grain boundaries of zinc is higher than that on the intra-crystallines of zinc, indicating that the growth of molybdate films at the grain boundaries of zinc is quicker than that on the intra-crystallines of zinc. This is similar to the growth of the single molybdate films on the surface of HDG steel[9].

Table 2 Chemical composition of different micro-sites corresponding to Fig.1 (mass fraction, %)

Micro-site	Element			
	O	P	Mo	Zn
Site 1	25.26	12.52	2.10	60.11
Site 2	14.31	5.41	3.02	77.26
Site 3	6.41	2.43	1.34	89.81

When the phosphated and molybdate post-sealed HDG samples are finally rinsed with water thoroughly,

the element of Mo on the surface of the needle-like zinc phosphate crystals is not detected. This may be due to that the element of Mo on the zinc phosphate crystals is the condensed molybdate compounds that are carried over from the molybdate solution when the samples are finally withdrawn from sodium molybdate solution. In Fig.2, the molybdate particles absorbed on the needle-like zinc phosphate crystals are clearer. After rinsing the samples, the absorbed molybdate salts were washed away. Therefore, the element of Mo on the needle-like zinc phosphate crystals is absent.

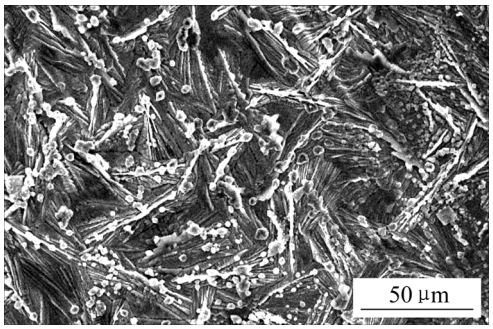

Fig.2 SEM micrograph of molybdate particles on needle-like zinc phosphate crystals

Fig.3 shows the SEM micrographs of the 5-min phosphated HDG samples without and with molybdate post-sealing treatment. After post-sealing the phosphated HDG samples with molybdate solution, the surface morphology of the coatings appears to be unchanged. The needle-like zinc phosphate crystals are still obvious and take up a most great part of the zinc layer (Fig.3(b)).

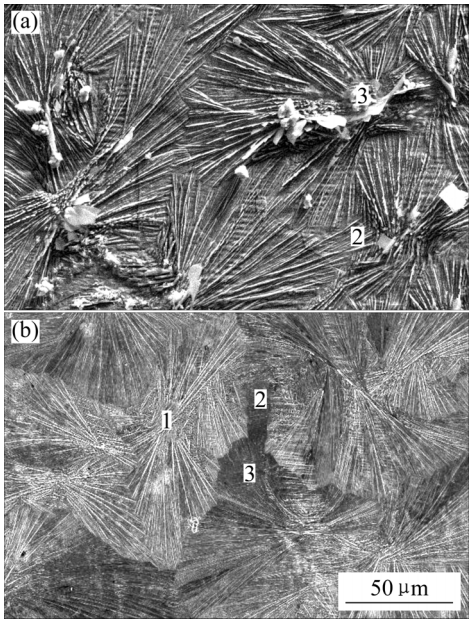

Fig.3 SEM micrographs of 5 min phosphated HDG samples: (a) Without post-sealing; (b) Post-sealing with molybdate solution for 50 s

The chemical composition of different micro-sites corresponding to Fig.3 is listed in Table 3. The contents of P and O on the bigger wafers (site 1 of Fig.3(a)) are higher, whereas that of O is less and the element of P is not detected on the pores among the needle-like zinc phosphate crystals (site 2 of Fig.3(a)). It is revealed that the zinc phosphate crystals cannot cover the surface of zinc completely and the pores are the exposed zinc layers.

After post-sealing the phosphated HDG samples with molybdate solution, besides the cores of the needle-like zinc phosphate crystals (site 1 of Fig.3(b)), both the pores (site 2 of Fig.3(b)) and the peripheries of the zinc phosphate crystals (site 3 of Fig.3(b)) have the element of Mo. It is indicated that the pores among the needle-like phosphate crystals are sealed with molybdate films and the continuous composite coatings are formed on the surface of HDG steel. Moreover, the cracks that exist in the single molybdate films are not observed in the composite coatings[9].

Table 3 Chemical composition of different micro-sites corresponding to Fig.3 (mass fraction, %)

Fig.3	Micro-site	Element			
		O	P	Zn	Mo
(a)	Site 1	35.37	14.44	50.19	−
	Site 2	2.77	0	97.23	−
(b)	Site 1	23.81	15.52	60.67	0.00
	Site 2	5.13	1.80	92.09	0.99
	Site 3	18.66	10.15	70.94	0.26

3.2 Corrosion resistance of coatings

To sign the HDG samples with different treatments, the symbols are introduced as follows: HDG—untreated; Mo—only treated with molybdate solution for 50 s; P—only phosphated; and P+Mo—previously phosphated and subsequently sealed with molybdate solution for 50 s. The numbers behind P are the phosphating time (s).

Fig.4 shows the Tafel polarization curves for HDG, Mo, P and P+Mo immersed in 5% NaCl solution. The corresponding corrosion potential E_{corr}, current density J_{corr} and polarization resistance R_p obtained from the polarization curves by Tafel extrapolation method are listed in Table 4.

In the first 30 s of phosphating, the cathodic branch on the polarization curves for P30 is shifted markedly towards the direction where J_{corr} decreases, whereas that of the anodic branch is smaller, indicating the remarkable suppression of the cathodic process and the inconspicuous suppression of the anodic process of zinc corrosion(Fig.4(a)). This may be due to that the zinc phosphate crystals preferentially nucleate at the micro-cathodic active sites[17]. With the increase of

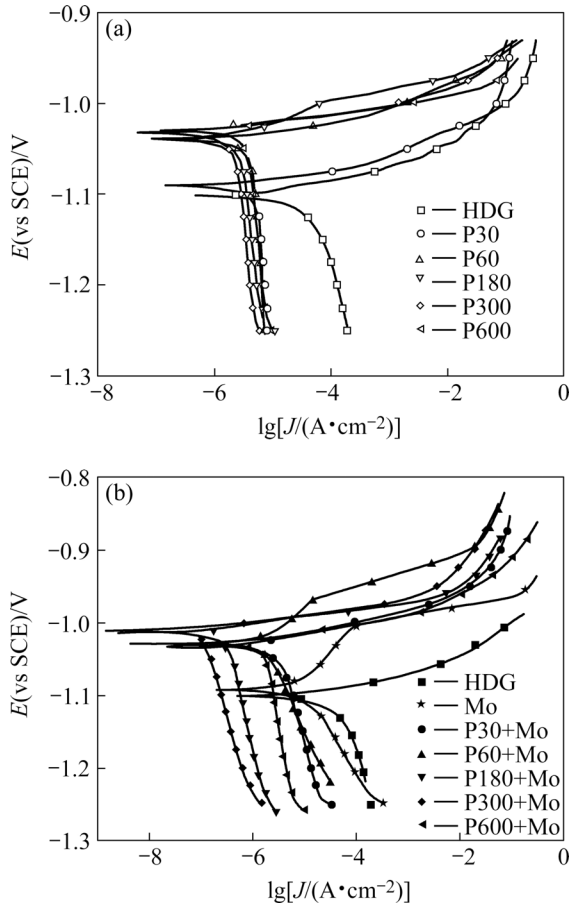

Fig.4 Tafel polarization curves for: (a) HDG and P; (b) HDG, Mo and P+Mo immersed in 5% NaCl solution

Table 4 Corrosion potential E_{corr}, current density J_{corr} and polarization resistance R_p obtained from polarization curves in Fig.4 by Tafel extrapolation method

Sample	E_{corr}(vs SCE)/ V	J_{corr}/ ($\mu A \cdot cm^{-2}$)	R_p/ ($k\Omega \cdot cm^2$)
HDG	−1.101	16.80	0.50
Mo	−1.092	6.64	1.80
P30	−1.092	5.33	1.36
P60	−1.043	3.56	1.68
P180	−1.037	2.06	4.05
P300	−1.032	1.67	4.55
P600	−1.030	1.36	5.46
P30+Mo	−1.032	1.32	4.50
P60+Mo	−1.029	1.29	7.60
P180+Mo	−1.014	0.10	31.60
P300+Mo	−1.010	0.08	49.50
P600+Mo	−1.012	0.10	32.30

phosphating time, the shift extent of the cathodic branches for P towards the direction where J_{corr} decreases is less; whereas the shift extent of the anodic branches is more on the whole, because of the gradual growth of the zinc phosphate crystals and the increases in coverage of the zinc layer.

The anodic and cathodic branches on the polarization curves for P+Mo are shifted evidently and evenly in the direction where J_{corr} decreases both at the initial stage and during the prolonged stage of phosphating on the whole (Fig.4(b)). It is suggested that the anodic and cathodic processes of zinc corrosion are suppressed conspicuously. Post-sealing the phosphated HDG samples with molybdate solution, the pores on phosphate coatings are sealed with molybdate films and the active sites on the zinc layer are decreased. Moreover, molybdate ions inhibit the anodic process of zinc corrosion by the formation of the zinc molybdate precipitates[8], resulting in the obvious shift of the anodic branches towards the direction where J_{corr} decreases at the initial stage of phosphating. With the increase in phosphating time, the pores on the composite coatings are diminished gradually and may be vanished eventually. The exposed zinc area in NaCl solution is thereby decreased significantly, and the diffusion of oxygen to the zinc layer becomes more and more difficult. Therefore, the anodic process of zinc dissolution and the cathodic process of oxygen reduction are suppressed markedly.

In Table 4, for P and P+Mo, the values of J_{corr} are decreased and those of R_p are increased with the increase in phosphating time. For the same phosphating time, the value of J_{corr} for P+Mo is significantly smaller than that for P or Mo, and the value of R_p of the former is markedly higher than that of the latter, even fairly higher than the summation of the two latter ones.

The corrosion protection efficiency, P_e of the coatings for HDG steel immersed in 5% NaCl solution was obtained by the following expression:

$$P_e = (1 - J_{corr} / J^0_{corr}) \times 100\% \quad (1)$$

where J^0_{corr} and J_{corr} are the corrosion current densities of the untreated and treated HDG samples, respectively. The P_e values for P and P+Mo calculated from Eqn.(1) and data in Table 4 are exhibited as a function of phosphating time in Fig.5. The P_e value for P+Mo is fairly higher than that for P when the phosphating time is the same.

Assuming that the two single coatings for suppressing zinc corrosion are independent, the corrosion protection efficiency of the composite coatings, $P_{e,c}$ could be stated as follows[18]:

$$P_{e,c}=P_{e,p}+P_{e,m}-P_{e,p} \times P_{e,m} \quad (2)$$

where $P_{e,p}$ and $P_{e,m}$ are the protection efficiency P_e of the single phosphate coatings and the single molybdate

films, respectively. The P_e value for Mo calculated from Eqn.(1) and data in Table 4 is 60.6%. The $P_{e,c}$ values for P+Mo calculated from Eqn.(2) are also shown in Fig.5. Apparently, the measured $P_{e,c}$ values are higher than the calculated ones. It is indicated that post-sealing the phosphated HDG steel with molybdate solution, the synergistic corrosion protection effect of the single phosphate coatings and the single molybdate films for zinc is exerted markedly.

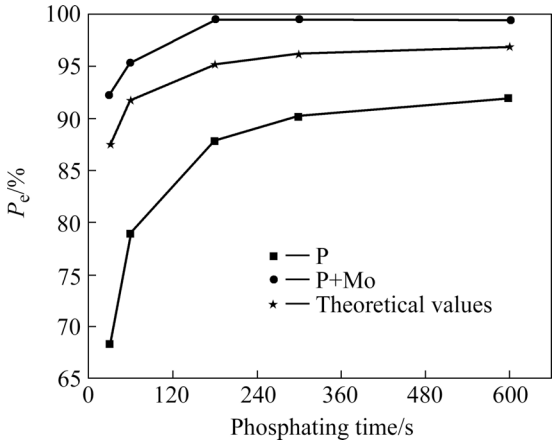

Fig.5 P_e values for P, P+Mo and theoretical ones as function of phosphating time

Fig.6 shows the NSS results of Mo, P and P+Mo phosphated for different times. For P and P+Mo, the corrosion resistance increases greatly with the increase in phosphating time up to 300 s, and subsequently the variation of the corrosion resistance with phosphating time is inconspicuous. For the same phosphating time, the corroded area of zinc on P+Mo is fairly smaller than that on P. The composite coatings with optimal corrosion resistance are obtained for pre-phosphating 300 s and post-sealing with molybdate solution for 50 s, on which no corrosion is observed in five spray cycles; whereas the corrosion appears on the single phosphate coatings in only one spray cycle and the corroded area of zinc on Mo

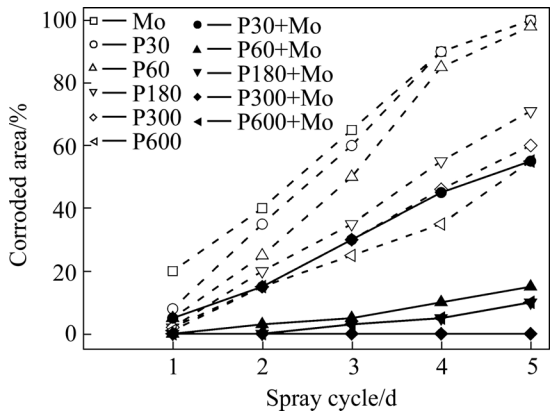

Fig.6 NSS results of Mo, P and P+Mo

is larger, around 20% in only one spray cycle. The corroded area of zinc on HDG is the largest, more than 95% after 8 h spray. This is in agreement with the results of the Tafel polarization measurements.

4 Conclusions

1) After post-sealing the phosphated HDG samples with sodium molybdate solution, the pores among the zinc phosphate crystals are sealed with molybdate films containing Zn, P, O and Mo, and the continuous composite coatings are formed on HDG steel.

2) Both the anodic process and the cathodic process of zinc corrosion on the samples are suppressed more conspicuously. For the same phosphating time, the corrosion current density of the composite coatings is fairly smaller than that of the single phosphate coatings or molybdate films; the polarization resistance of the former is significantly higher than that of the latter, even significantly larger than the summation of the two latter ones.

3) The synergistic corrosion protection effect of the single phosphate coatings and the single molybdate films is exerted markedly.

4) The composite coatings with optimal corrosion resistance are obtained for pre-phosphating 300 s and subsequently post-sealed with molybdate solution for 50 s, and no corrosion is observed in five spray cycles.

References

[1] LORIN G. Phosphating of metals: constitution, physical chemistry and technical applications of phosphating solutions [M]. Hampton Hill: Finishing Publications, 1974: 146−155.

[2] FREEMAN D B. Phosphating and metal pre-treatment [M]. New York: Industrial Press, 1986: 134−139.

[3] RAUSCH W. The phosphating of metals [M]. Ohio: ASM International, 1990: 112−116.

[4] SUSAC D, LEUNG C W, SUN X, WONG K C, MITCHELL K A R. Comparison of a chromic acid and a BTSE final rinse applied to phosphated 2024-T3 aluminum alloy [J]. Surf Coat Technol, 2004, 187(2/3): 216−224.

[5] SHIGEYOSHI M, MASAHIRO Y. The role of chromate treatment after phosphating in paint adhesion [J]. Prog Org Coat, 1998, 33(1): 83−89.

[6] NIE Tang, WIM J O, GEORGE G. Comparative EIS study of pretreatment performance in coated metals [J]. Progress in Organic Coatings, 1997, 30(4): 255−263.

[7] VUKASOVICH M S, FARR J P G. Molybdatein corrosion inhibition—A review [J]. Mater Perform, 1986, 25(5): 9−18.

[8] ARAMAKI K. The inhibition effects of chromate-free, anion inhibitors on corrosion of zinc in aerated 0.5 mol/L NaCl [J]. Corros Sci, 2001, 43(3): 591−604.

[9] LU Jin-tang, KONG Gang, CHEN Jin-hong, XU Qiao-yu, SUI Run-zhou. Growth and corrosion behavior of molybate passivation film on hot dip galvanized steel [J]. Trans Nonferrous Met Soc China, 2003, 13(1): 145−148.

[10] WILCOX G D, GABE D R. Chemical molybdate conversion

treatments for zinc [J]. Met Finish, 1988, 86(9): 71−74.

[11] LI Guang-yu, NIU Li-yuan, LIAN Jian-she, JIANG Zhong-hao. A black phosphate coating for C1008 steel [J]. Surf Coat Technol, 2004, 176(2): 215−221.

[12] SALIBA-SILVA A M, DE OLIVEIRA M C L, COSTA I. Effect of molybdate on phosphating of Nd-Fe-B magnets for corrosion protection [J]. Mater Res Bull, 2005, 8(2): 147−150.

[13] LIN Bi-lan, LU Jin-tang, KONG Gang, LIU Jun. Growth and corrosion resistance of molybdate modified zinc phosphate conversion coatings on hot-dip galvanized steel [J]. Trans Nonferrous Met Soc China, 2007, 17(4): 755−761.

[14] LI Guang-yu, LIAN Jian-she, NIU Li-yuan, JIANG Zhong-hao, JIANG Qing. Preparation, structure and properties of molybdate modified zinc phosphate coating on magnesium alloy AZ91D [J]. Chemical Journal of Chinese University, 2006, 27(5): 817−820. (in Chinese)

[15] LIN Bi-lan, KONG Gang, LU Jin-tang, LIU Jun. Study of growth and corrosion resistance of zinc phosphate conversion coatings on hot dip galvanized steel [J]. The Chinese Journal of Nonferrous Metals, 2007, 17(5): 800−806. (in Chinese)

[16] NOTTER I M, GABE D R. Polarisation resistance methods for measurement of the porosity of thin metal coatings [J]. Corros Sci, 1993, 34(5): 851−870.

[17] SUSAC D, SUN X, LI R Y, WONG K C, WONG P C, MITCHELL K A R, CHAMPANERIA R. Microstructural effects on the initiation of zinc phosphate coatings on 2024-T3 aluminum alloy [J]. Appl Surf Sci, 2004, 239(1): 45−59.

[18] SUZUKI T, NISHIHARA H, ARAMAKI K. The synergistic inhibition effect of octylmercaptopropionate and 8-quinolinol on the corrosion of iron in an aerated 0.5 mol/L Na_2SO_4 solution [J]. Corros Sci, 1996, 38(8): 1223−1234.

(Edited by CHEN Wei-ping)